

# Transverse-momentum distributions of hadrons produced in DIS at COMPASS

Jan Matoušek

Charles University, Prague, Czechia  
on behalf of the COMPASS collaboration



CHARLES UNIVERSITY  
Faculty of mathematics  
and physics



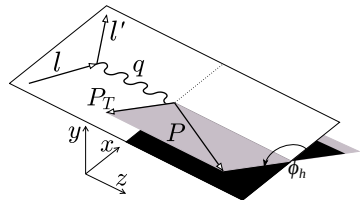


The cross section for producing a hadron  $h$  in DIS on unpolarised target  $\ell N \rightarrow \ell' h X$ :

[A. Bacchetta *et al.*, JHEP 0702 (2007)]

$$\begin{aligned} \frac{d\sigma}{dxdydzd\phi_h dP_T^2} = & \frac{2\pi\alpha^2}{xyQ^2} \frac{y^2}{2(1-\varepsilon)} \left(1 + \frac{2xM^2}{Q^2}\right) \left( F_{UU,T} + \varepsilon F_{UU,L} \right. \\ & \left. + \sqrt{2\varepsilon(1+\varepsilon)} F_{UU}^{\cos \phi_h} \cos \phi_h + \varepsilon F_{UU}^{\cos 2\phi_h} \cos 2\phi_h + \lambda \sqrt{2\varepsilon(1-\varepsilon)} F_{LU}^{\sin \phi_h} \sin \phi_h \right) \\ = & \sigma_0 \left( 1 + \varepsilon_1 A_{UU}^{\cos \phi_h} \cos \phi_h + \varepsilon_2 A_{UU}^{\cos 2\phi_h} \cos 2\phi_h + \lambda \varepsilon_3 A_{LU}^{\sin \phi_h} \sin \phi_h \right) \end{aligned}$$

- where  $x, y, Q^2$  are usual DIS variables,
- $\lambda$  is the beam polarisation ( $\approx 0.8$  at COMPASS),
- $z$  is the fraction of  $\gamma^*$  energy carried by  $h$ .
- $P_T$  is the transverse momentum of  $h$  in the  $\gamma N$  frame,  $\phi_h$  is its azimuthal angle.
- $F_{XU}^{f(\phi_h)}(x, z, P_T^2, Q^2)$  are structure functions.
- $A_{XU}^{f(\phi_h)}(x, z, P_T^2, Q^2)$  are commonly called azimuthal asymmetries.



SIDIS in the  $\gamma$ -nucleon frame.

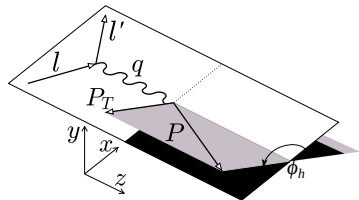


The cross section for producing a hadron  $h$  in DIS on unpolarised target  $\ell N \rightarrow \ell' h X$ :

[A. Bacchetta *et al.*, JHEP 0702 (2007)]

$$\begin{aligned} \frac{d\sigma}{dxdydzd\phi_h dP_T^2} &= \frac{2\pi\alpha^2}{xyQ^2} \frac{y^2}{2(1-\varepsilon)} \left(1 + \frac{2xM^2}{Q^2}\right) \left( F_{UU,T} + \varepsilon F_{UU,L} \right. \\ &\quad \left. + \sqrt{2\varepsilon(1+\varepsilon)} F_{UU}^{\cos \phi_h} \cos \phi_h + \varepsilon F_{UU}^{\cos 2\phi_h} \cos 2\phi_h + \lambda \sqrt{2\varepsilon(1-\varepsilon)} F_{LU}^{\sin \phi_h} \sin \phi_h \right) \\ &= \sigma_0 \left( 1 + \varepsilon_1 A_{UU}^{\cos \phi_h} \cos \phi_h + \varepsilon_2 A_{UU}^{\cos 2\phi_h} \cos 2\phi_h + \lambda \varepsilon_3 A_{LU}^{\sin \phi_h} \sin \phi_h \right) \end{aligned}$$

- where  $x, y, Q^2$  are usual DIS variables,
- $\lambda$  is the beam polarisation ( $\approx 0.8$  at COMPASS),
- $z$  is the fraction of  $\gamma^*$  energy carried by  $h$ .
- $P_T$  is the transverse momentum of  $h$  in the  $\gamma N$  frame,  $\phi_h$  is its azimuthal angle.
- $F_{XU}^{f(\phi_h)}(x, z, P_T^2, Q^2)$  are structure functions.
- $A_{XU}^{f(\phi_h)}(x, z, P_T^2, Q^2)$  are commonly called azimuthal asymmetries.



SIDIS in the  $\gamma$ -nucleon frame.



The unpolarised structure function in terms of TMD PDFs and TMD FFs:

$$F_{UU,T} = \mathcal{C} [f_1 D_1],$$

Gaussian ansatz:

$$f_1^q(x, k_T^2) = f_1^q(x) \frac{1}{\pi \langle k_{Tq}^2 \rangle} e^{-\frac{k_T^2}{\langle k_{Tq}^2 \rangle}}$$

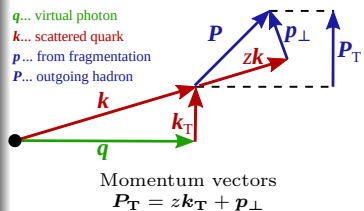
$$D_1^{h/q}(z, p_\perp^2) = D_1^{h/q}(z) \frac{1}{\pi \langle p_{\perp h/q}^2 \rangle} e^{-\frac{p_\perp^2}{\langle p_{\perp h/q}^2 \rangle}}$$

Assuming flavour independence of  $\langle k_T^2 \rangle$  and  $\langle p_\perp^2 \rangle$ :

$$F_{UU,T} = x \sum_q e_q^2 f_1^q(x) D_1^{h/q}(z) \frac{1}{\pi \langle P_T^2 \rangle} e^{-\frac{P_T^2}{\langle P_T^2 \rangle}}$$

where

$$\langle P_T^2 \rangle = z^2 \langle k_{Tq}^2 \rangle + \langle p_{\perp h/q}^2 \rangle.$$



- $f_1(x, k_T^2, Q^2)$  unpolarised TMD PDF,
- $D_1(z, p_\perp^2, Q^2)$  unpolarised TMD FF,
- $\mathcal{C}$  = sum over flavours and convolution over  $\mathbf{p}_\perp, \mathbf{k}_T$ ,



The unpolarised structure function in terms of TMD PDFs and TMD FFs:

$$F_{UU,T} = \mathcal{C} [f_1 D_1],$$

Gaussian ansatz:

$$f_1^q(x, k_T^2) = f_1^q(x) \frac{1}{\pi \langle k_{Tq}^2 \rangle} e^{-\frac{k_T^2}{\langle k_{Tq}^2 \rangle}}$$

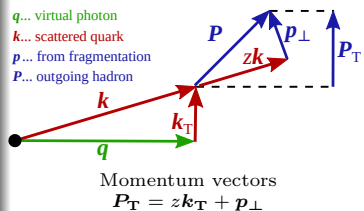
$$D_1^{h/q}(z, p_\perp^2) = D_1^{h/q}(z) \frac{1}{\pi \langle p_{\perp h/q}^2 \rangle} e^{-\frac{p_\perp^2}{\langle p_{\perp h/q}^2 \rangle}}$$

Assuming flavour independence of  $\langle k_T^2 \rangle$  and  $\langle p_\perp^2 \rangle$ :

$$F_{UU,T} = x \sum_q e_q^2 f_1^q(x) D_1^{h/q}(z) \frac{1}{\pi \langle P_T^2 \rangle} e^{-\frac{P_T^2}{\langle P_T^2 \rangle}}$$

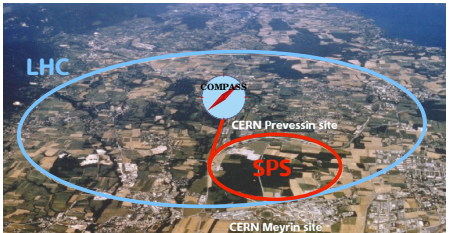
where

$$\langle P_T^2 \rangle = z^2 \langle k_{Tq}^2 \rangle + \langle p_{\perp h/q}^2 \rangle.$$



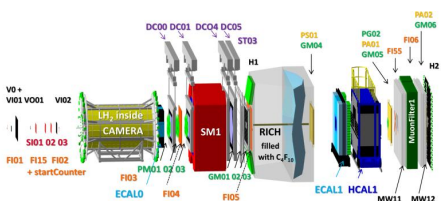
- $f_1(x, k_T^2, Q^2)$  unpolarised TMD PDF,
- $D_1(z, p_\perp^2, Q^2)$  unpolarised TMD FF,
- $\mathcal{C}$  = sum over flavours and convolution over  $p_\perp, k_T$ ,

# Introduction: COMPASS



It is located at M2 beamline of CERN's SPS.

- Collaboration: 24 institutes, 13 countries.
- Fixed target, multi-purpose.
- Broad research programme:
  - **SIDIS:**  $\mu^+$  beam and L/T-polarised proton ( $\text{NH}_3$ ) or deuteron ( ${}^6\text{LiD}$ ) target (beam 160 GeV/c, 200 GeV/c in 2011)  
**Summary by F. Bradamante on Monday.**
  - **Hadron spectroscopy:** hadron beams and nuclear targets.
  - **Drell-Yan:** 190 GeV/c  $\pi^-$  beam and  $p^\uparrow$ , Al and W targets – **R. Longo, Friday.**
  - **Hard exclusive processes and SIDIS:** 160 GeV/c  $\mu^\pm$  beam and liquid  $\text{H}_2$  target.  
**DVCS & HEMP – N. d'Hose, Wednesday.**



2016–2017 setup with CAMERA recoil proton detector and ECAL0 calorimeter for DVCS studies.



## Published unpolarised SIDIS results:

- Azimuthal asymmetries on  ${}^6\text{LiD}$  target [COMPASS, Nucl.Phys.B 886 (2014)].
- $P_{\text{T}}$ -dependent multiplicities on  ${}^6\text{LiD}$  target [COMPASS, Phys.Rev.D97 (2018)]
- Background to the asymmetries from decays of exclusive vector mesons [COMPASS, Nucl.Phys.B 956 (2020)].

## Ongoing analysis presented in this talk:

- 2016–2017 data taken with 2.5 m long  $\text{LH}_2$  target.
- Primary goal: exclusive measurements, useful for SIDIS as well.
- Advantages:
  - pure proton target,
  - alternating  $\mu^{\pm}$  beam with balanced statistics (stability tests for systematics),
  - MC development in synergy with DVCS analysis.
- Part of the data (about 11 %) used for these preliminary results.
- $P_{\text{T}}^2$ -distributions – this talk.
- Azimuthal asymmetries – A. Moretti (next talk).

## Future:

- 2022 run with  ${}^6\text{LiD}$  target (transversely polarised).



## Published unpolarised SIDIS results:

- Azimuthal asymmetries on  ${}^6\text{LiD}$  target [COMPASS, Nucl.Phys.B 886 (2014)].
- $P_{\text{T}}$ -dependent multiplicities on  ${}^6\text{LiD}$  target [COMPASS, Phys.Rev.D97 (2018)]
- Background to the asymmetries from decays of exclusive vector mesons [COMPASS, Nucl.Phys.B 956 (2020)].

## Ongoing analysis presented in this talk:

- 2016–2017 data taken with 2.5 m long  $\text{LH}_2$  target.
- Primary goal: exclusive measurements, useful for SIDIS as well.
- Advantages:
  - pure proton target,
  - alternating  $\mu^\pm$  beam with balanced statistics (stability tests for systematics),
  - MC development in synergy with DVCS analysis.
- Part of the data (about 11 %) used for these preliminary results.
- $P_{\text{T}}^2$ -distributions – this talk.
- **Azimuthal asymmetries – A. Moretti (next talk).**

## Future:

- 2022 run with  ${}^6\text{LiD}$  target (transversely polarised).



## Published unpolarised SIDIS results:

- Azimuthal asymmetries on  ${}^6\text{LiD}$  target [COMPASS, Nucl.Phys.B 886 (2014)].
- $P_{\text{T}}$ -dependent multiplicities on  ${}^6\text{LiD}$  target [COMPASS, Phys.Rev.D97 (2018)]
- Background to the asymmetries from decays of exclusive vector mesons [COMPASS, Nucl.Phys.B 956 (2020)].

## Ongoing analysis presented in this talk:

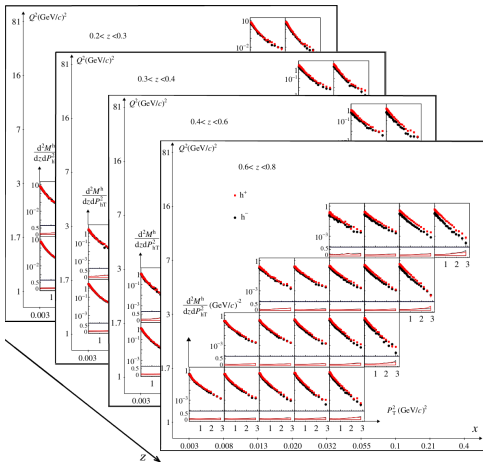
- 2016–2017 data taken with 2.5 m long  $\text{LH}_2$  target.
- Primary goal: exclusive measurements, useful for SIDIS as well.
- Advantages:
  - pure proton target,
  - alternating  $\mu^{\pm}$  beam with balanced statistics (stability tests for systematics),
  - MC development in synergy with DVCS analysis.
- Part of the data (about 11 %) used for these preliminary results.
- $P_{\text{T}}^2$ -distributions – this talk.
- Azimuthal asymmetries – A. Moretti (next talk).

## Future:

- 2022 run with  ${}^6\text{LiD}$  target (transversely polarised).

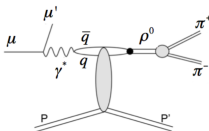
# Measurement on ${}^6\text{LiD}$ :

- [COMPASS, Phys. Rev. D97 (2018)]
- 4D analysis  
(bins in  $x$ ,  $Q^2$ ,  $z$  and  $P_T^2$ )
- Unidentified charged hadrons studied.
- QED radiative effects taken into account.
- Contribution of the decay of exclusive vector mesons
  - Contamination estimated from HEPGEN MC generator  
[A. Sandacz & P. Sznajder, arXiv:1207.0333].
  - Subtracted in each bin.
  - $\rho^0$ : small  $P_T$ , large  $z$ , small  $Q^2$ .
  - $\phi$ : tiny  $P_T$ , medium  $z$ , small  $Q^2$ .

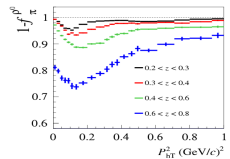


# Measurement on ${}^6\text{LiD}$ :

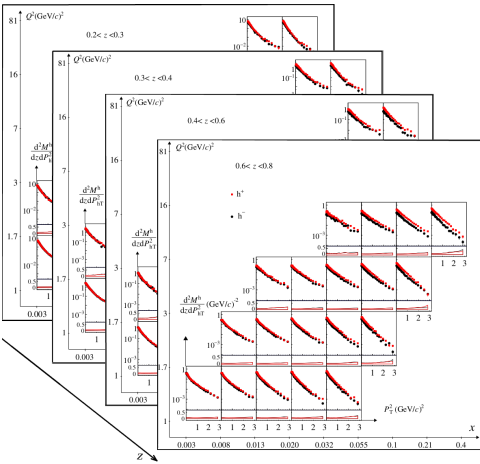
- [COMPASS, Phys. Rev. D97 (2018)]
- 4D analysis  
(bins in  $x$ ,  $Q^2$ ,  $z$  and  $P_T^2$ )
- Unidentified charged hadrons studied.
- QED radiative effects taken into account.
- Contribution of the decay of exclusive vector mesons
  - Contamination estimated from HEPGEN MC generator  
[A. Sandacz & P. Sznajder, arXiv:1207.0333].
  - Subtracted in each bin.
  - $\rho^0$ : small  $P_T$ , large  $z$ , small  $Q^2$ .
  - $\phi$ : tiny  $P_T$ , medium  $z$ , small  $Q^2$ .

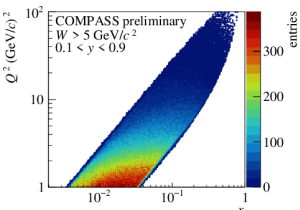
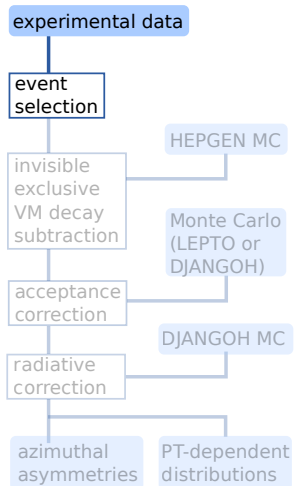


Diffractively produced  $\rho^0 \rightarrow \pi^+\pi^-$ , creating a background to SIDIS.



$1 - \rho^0$  contamination fraction.





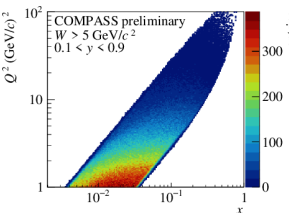
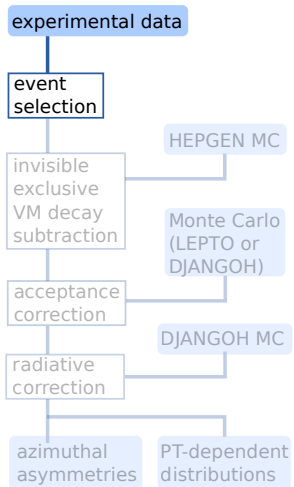
The  $x$  and  $Q^2$  range covered.

## DIS event selection

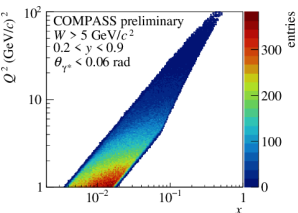
- $Q^2 > 1 \text{ (GeV}/c\text{)}^2$ ,
- $W > 5 \text{ GeV}/c^2$ ,
- $0.003 < x < 0.13$ ,
- $0.2 < y < 0.9$ ,
- $\theta_\gamma < 60 \text{ mrad}$ ,
- Exclusive VM decay cut:  
if only  $\mu^+ h^+ h^-$  outgoing,  
 $z_1 + z_2 = z_t < 0.95$ .

## Hadron selection

- $0.1 < z < 0.85$ ,
- $0.1 < P_T/(\text{GeV}/c) < 1.73$ .



The  $x$  and  $Q^2$  range covered.



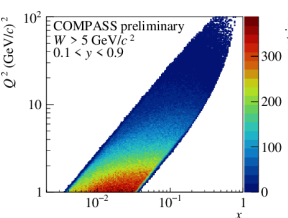
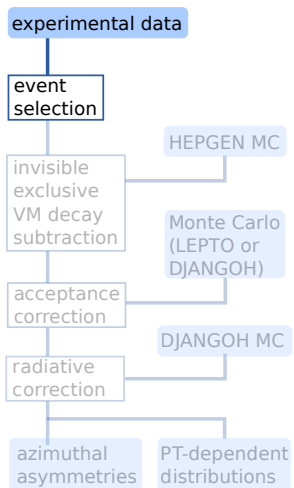
Selected range with moderate acceptance corrections.

## DIS event selection

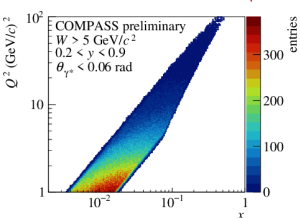
- $Q^2 > 1 \text{ (GeV}/c)^2$ ,
- $W > 5 \text{ GeV}/c^2$ ,
- $0.003 < x < 0.13$ ,
- $0.2 < y < 0.9$ ,
- $\theta_\gamma < 60 \text{ mrad}$ ,
- Exclusive VM decay cut:  
if only  $\mu^+ h^+ h^-$  outgoing,  
 $z_1 + z_2 = z_t < 0.95$ .

## Hadron selection

- $0.1 < z < 0.85$ ,
- $0.1 < P_T/(\text{GeV}/c) < 1.73$ .



The  $x$  and  $Q^2$  range covered.



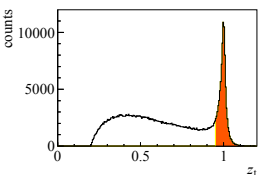
Selected range with moderate acceptance corrections.

## DIS event selection

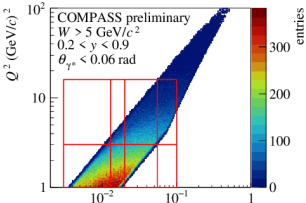
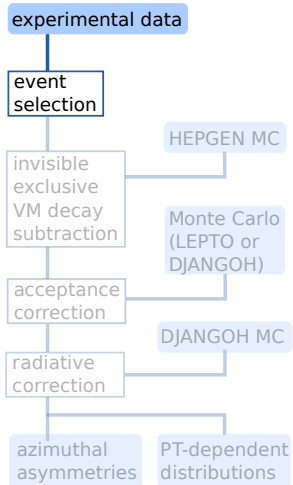
- $Q^2 > 1 \text{ (GeV}/c)^2$ ,
- $W > 5 \text{ GeV}/c^2$ ,
- $0.003 < x < 0.13$ ,
- $0.2 < y < 0.9$ ,
- $\theta_\gamma < 60 \text{ mrad}$ ,
- Exclusive VM decay cut:  
if only  $\mu' h^+ h^-$  outgoing,  
 $z_1 + z_2 = z_t < 0.95$ .

## Hadron selection

- $0.1 < z < 0.85$ ,
- $0.1 < P_T/(\text{GeV}/c) < 1.73$ .



[COMPASS, Nucl. Phys. B 956 (2020)]

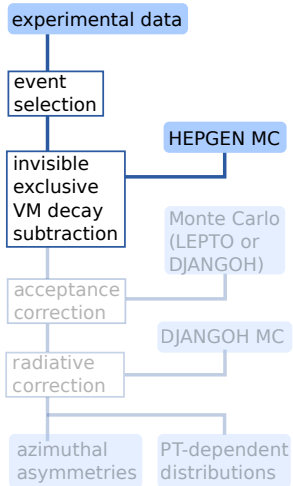


$Q^2$  and  $x$  bins for the  $P_T$ -dependent distributions.

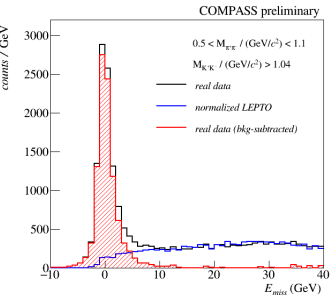
## Binning

- Based on the published results on  ${}^6\text{LiD}$ .
- Asymmetries:
  - 1D in  $x$ ,  $z$  and  $P_T$ .
  - 3D in  $x$ ,  $z$  and  $P_T$
- $P_T$ -dependent distributions
  - 4D in  $x$ ,  $Q^2$ ,  $z$  and  $P_T^2$ .
  - Larger bins w.r.t the publication
    - $4x \times 2Q^2 \times 4z$
    - $4x \times 2Q^2 \times 7z$
  - Additional binning in  $W$ 
    - $4x \times 3Q^2 \times 4z \times 2W$

# Measurement on LH<sub>2</sub>: Exclusive VM decay subtraction

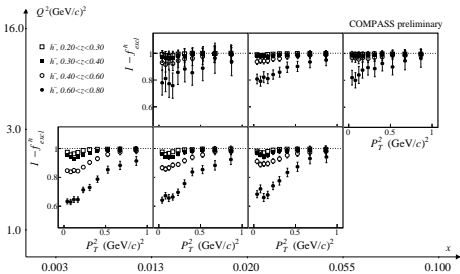
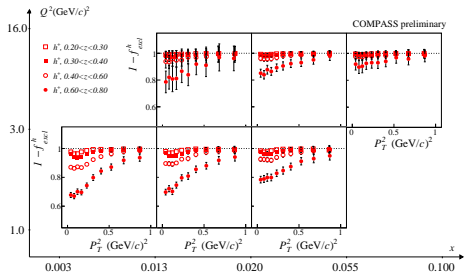


- Different approach w.r.t published d asymmetries.
- ‘Visible’ exclusive  $h^+h^-$  removed in event selection.
  - About 80 % of the decays are ‘visible’.
- ‘Invisible’ decays (only one h observed)
  - HEPGEN MC generator with azimuthal modulations.
  - Normalised to the data using  $E_{\text{miss}}$  distribution of the ‘visible’ decays.
  - Subtracted in every bin.



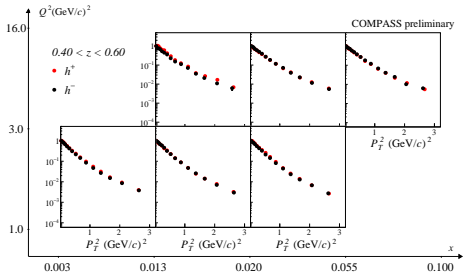
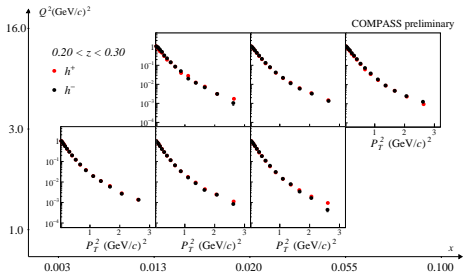
The number of signal events in the peak after SIDIS (from LEPTO) background subtraction is used to normalise HEPGEN.

Measurement on LH<sub>2</sub>: Exclusive VM decay subtraction



The impact of the VM-subtraction (the sum of ‘visible’ and ‘invisible’) on the  $P_T$ -dependent distributions.

# Measurement on LH<sub>2</sub>: Results for the $P_T$ -distributions



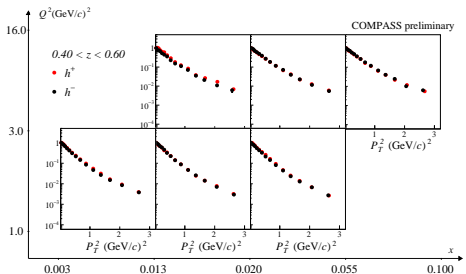
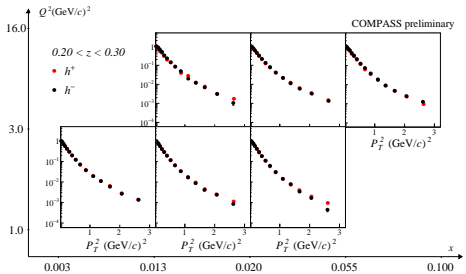
- Distributions normalised to the first bin.
- The shape almost the same for  $h^\pm$ 
  - no sign of flavour dependence of  $k_T$ ,  $p_\perp$ .
- Clear  $z$  and  $Q^2$  dependence.
- Gaussian model for  $f_1$  and  $D_1$ :

$$\frac{d^2N}{dz dP_T} \propto \exp\left(-\frac{P_T^2}{\langle P_T^2 \rangle}\right)$$

$$\langle P_T^2 \rangle = z^2 \langle k_T^2 \rangle + \langle p_\perp^2 \rangle.$$

- Deviation from the simple exponential visible at  $P_T > 1$  ( $\text{GeV}/c$ )<sup>2</sup>.

# Measurement on LH<sub>2</sub>: Results for the $P_T$ -distributions

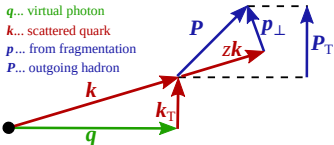


- Distributions normalised to the first bin.
- The shape almost the same for  $h^\pm$   
– no sign of flavour dependence of  $k_T$ ,  $p_\perp$ .
- Clear  $z$  and  $Q^2$  dependence.
- Gaussian model for  $f_1$  and  $D_1$ :

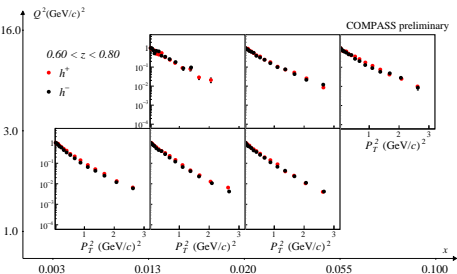
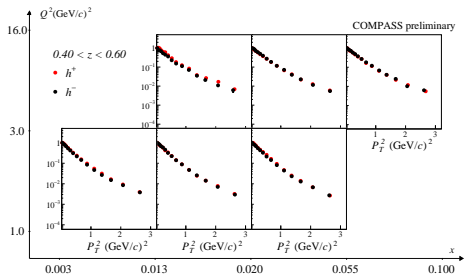
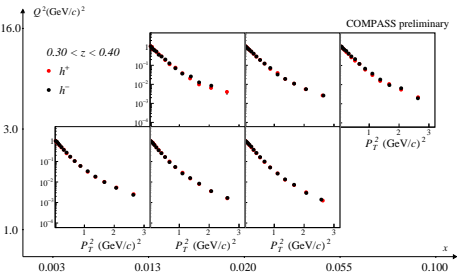
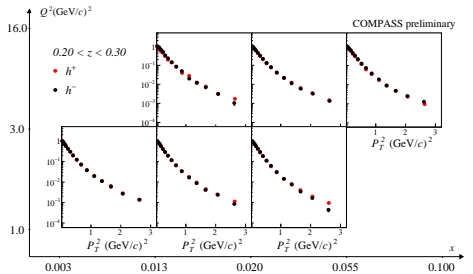
$$\frac{d^2N}{dz dP_T} \propto \exp\left(-\frac{P_T^2}{\langle P_T^2 \rangle}\right)$$

$$\langle P_T^2 \rangle = z^2 \langle k_T^2 \rangle + \langle p_\perp^2 \rangle.$$

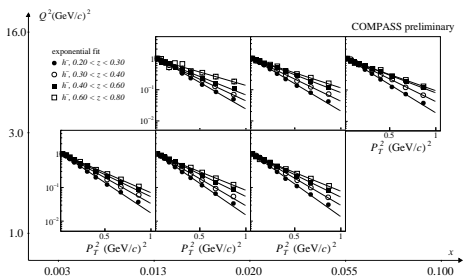
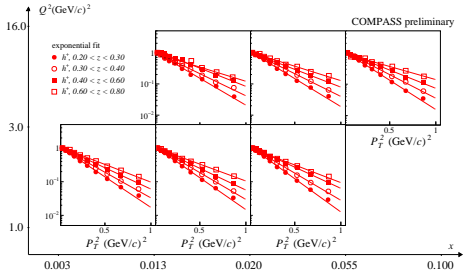
- Deviation from the simple exponential visible at  $P_T > 1$  ( $\text{GeV}/c$ )<sup>2</sup>.



# Measurement on LH<sub>2</sub>: Results for the $P_T$ -distributions



# Measurement on LH<sub>2</sub>: Results for the $P_T$ -distributions



Exponential fit in  $P_T < 1 (\text{GeV}/c)^2$  range.

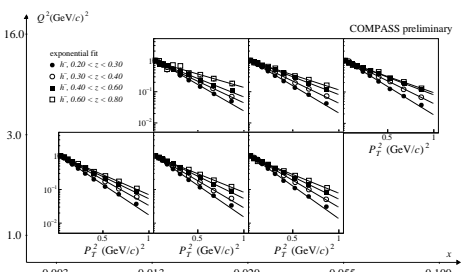
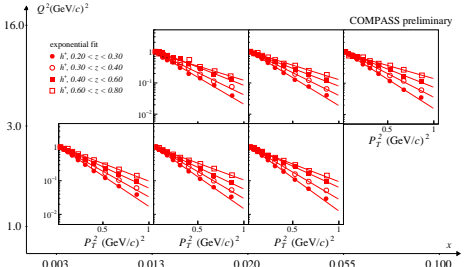
$$\frac{d^2N}{dz dP_T} \propto \exp\left(-\frac{P_T^2}{\langle P_T^2 \rangle}\right)$$

- Linear trend in  $z^2$  expected from the simple Gaussian model

$$\langle P_T^2 \rangle = z^2 \langle k_T^2 \rangle + \langle p_\perp^2 \rangle.$$

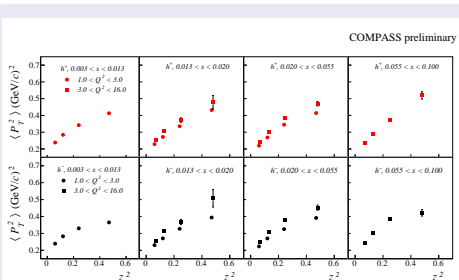
- Possible dependence of  $\langle p_\perp^2 \rangle$  on  $z$  or of  $\langle k_T^2 \rangle$  on  $x$ .
- Momentum conserv.:  $P_T \rightarrow 0$  at  $z \rightarrow 1$ .

# Measurement on LH<sub>2</sub>: Results for the $P_T$ -distributions



Exponential fit in  $P_T < 1 (\text{GeV}/c)^2$  range.

$$\frac{d^2N}{dz dP_T} \propto \exp\left(-\frac{P_T^2}{\langle P_T^2 \rangle}\right)$$



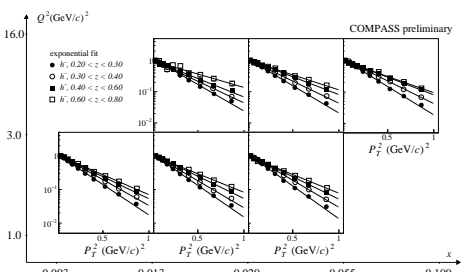
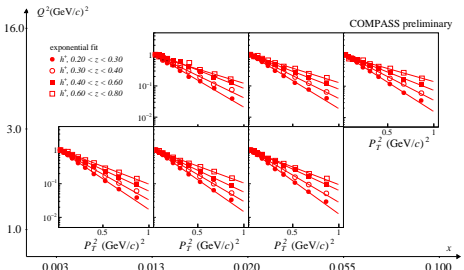
The fitted  $\langle P_T^2 \rangle$  versus  $z^2$  in the  $x$  and  $Q^2$  bins.

- Linear trend in  $z^2$  expected from the simple Gaussian model

$$\langle P_T^2 \rangle = z^2 \langle k_T^2 \rangle + \langle p_\perp^2 \rangle.$$

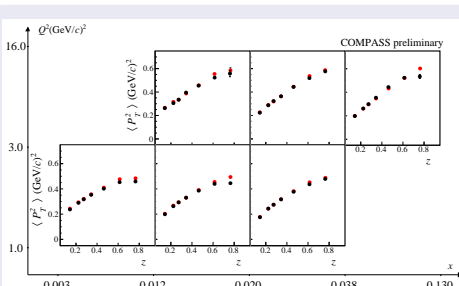
- Possible dependence of  $\langle p_\perp^2 \rangle$  on  $z$  or of  $\langle k_T^2 \rangle$  on  $x$ .
- Momentum conserv.:  $P_T \rightarrow 0$  at  $z \rightarrow 1$ .

# Measurement on LH<sub>2</sub>: Results for the $P_T$ -distributions



Exponential fit in  $P_T < 1$  ( $\text{GeV}/c^2$ ) range.

$$\frac{d^2N}{dz dP_T} \propto \exp\left(-\frac{P_T^2}{\langle P_T^2 \rangle}\right)$$



The fitted  $\langle P_T^2 \rangle$  versus  $z$  in the  $x$  and  $Q^2$  bins.

- Linear trend in  $z^2$  expected from the simple Gaussian model

$$\langle P_T^2 \rangle = z^2 \langle k_T^2 \rangle + \langle p_\perp^2 \rangle.$$

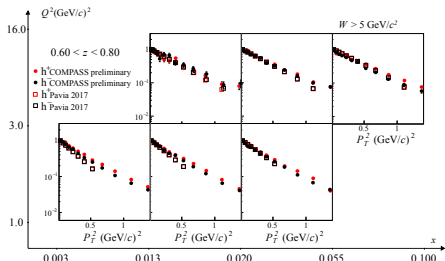
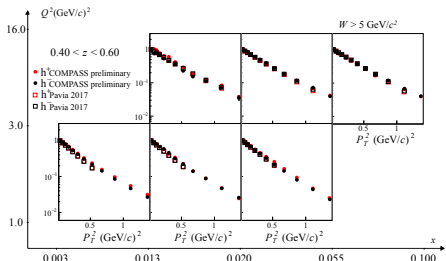
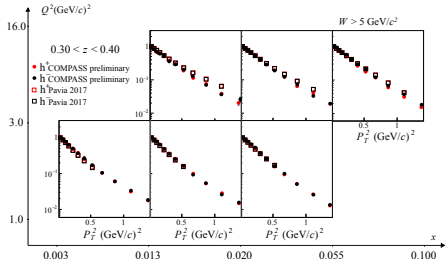
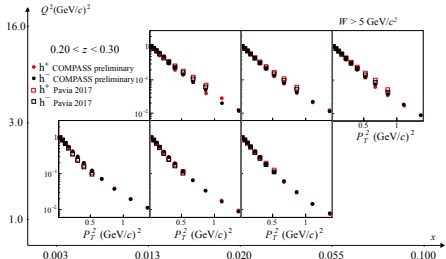
- Possible dependence of  $\langle p_\perp^2 \rangle$  on  $z$  or of  $\langle k_T^2 \rangle$  on  $x$ .
- Momentum conserv.:  $P_T \rightarrow 0$  at  $z \rightarrow 1$ .

# Measurement on LH<sub>2</sub>: Results for the $P_T$ -distributions

## Comparison with Pavia 2017 fit [A. Bacchetta *et al.*, JHEP 06 (2017) 081]

- SIDIS  $e p(D) \rightarrow e \pi^\pm (K^\pm) X$  (HERMES)
- SIDIS  $\mu D \rightarrow \mu h X$  (COMPASS)

- Drell-Yan (E228, E605)
- Z boson production (CDF, D0)

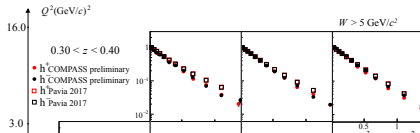
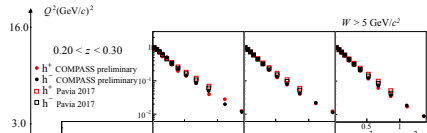


# Measurement on LH<sub>2</sub>: Results for the $P_T$ -distributions

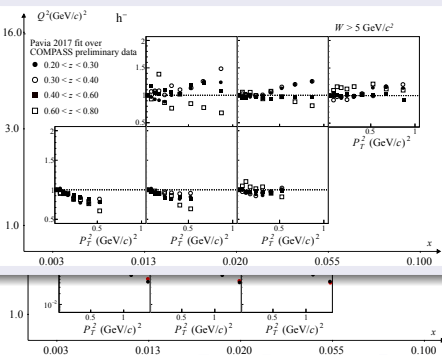
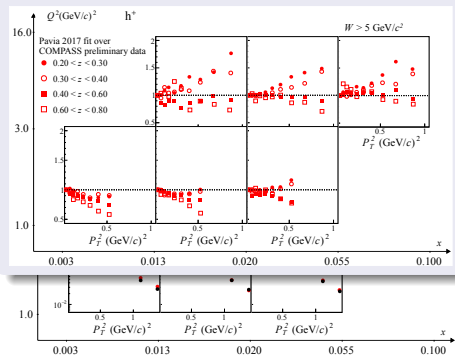
## Comparison with Pavia 2017 fit [A. Bacchetta *et al.*, JHEP 06 (2017) 081]

- SIDIS  $e p(D) \rightarrow e \pi^\pm (K^\pm) X$  (HERMES)
- SIDIS  $\mu D \rightarrow \mu h X$  (COMPASS)

- Drell-Yan (E228, E605)
- Z boson production (CDF, D0)



The ratio of the prediction from the fit over the preliminary data:





# Conclusion

## Interesting observables in unpolarised SIDIS

- Azimuthal asymmetries: sensitive to  $k_T$  (via Cahn effect) and to Boer–Mulders function.
- 2h-asymmetries – additional information on Boer–Mulders and Cahn.
- $P_T$ -dependent distributions: sensitive to  $k_T$  and  $p_\perp$  dependence of  $f_1$  and  $D_1$ .
- Contamination from decays of exclusive VMs – an important role in some regions.

## COMPASS measurements

- Published results on  ${}^6\text{LiD}$  target: [COMPASS, Nucl.Phys.B 886 (2014)], [COMPASS, Phys.Rev.D97 (2018)], [COMPASS, Nucl.Phys.B 956 (2020)].
- New preliminary results (August 2020) on liquid  $\text{H}_2$  target.
  - 11 % of the statistics,
  - More robust method for exclusive VM subtraction.
  - Alternating  $\mu^\pm$  beam – systematic check.
  - Qualitative agreement with deuteron.
  - Two-exponential shape, the same for  $h^\pm$ .
  - More results will come.
- 2022 measurement with (transversely polarised)  ${}^6\text{LiD}$  target just about to start.

These measurements provide important input to general understanding of the transverse-momentum-dependent structure of the nucleon and of the fragmentation process.



# Conclusion

## Interesting observables in unpolarised SIDIS

- Azimuthal asymmetries: sensitive to  $k_T$  (via Cahn effect) and to Boer–Mulders function.
- 2h-asymmetries – additional information on Boer–Mulders and Cahn.
- $P_T$ -dependent distributions: sensitive to  $k_T$  and  $p_\perp$  dependence of  $f_1$  and  $D_1$ .
- Contamination from decays of exclusive VMs – an important role in some regions.

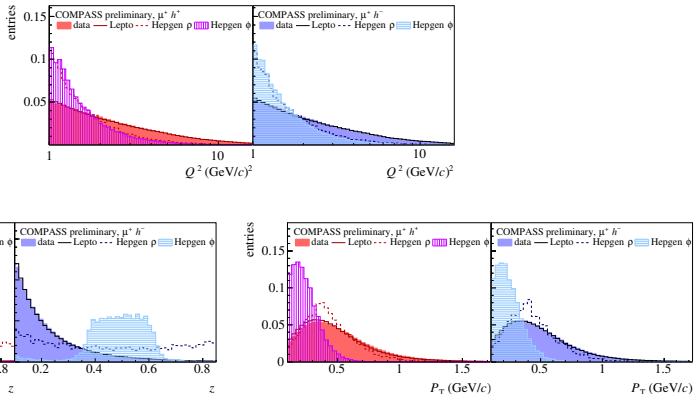
## COMPASS measurements

- Published results on  ${}^6\text{LiD}$  target: [COMPASS, Nucl.Phys.B 886 (2014)], [COMPASS, Phys.Rev.D97 (2018)], [COMPASS, Nucl.Phys.B 956 (2020)].
- New preliminary results (August 2020) on liquid  $\text{H}_2$  target.
  - 11 % of the statistics,
  - More robust method for exclusive VM subtraction.
  - Alternating  $\mu^\pm$  beam – systematic check.
  - Qualitative agreement with deuteron.
  - Two-exponential shape, the same for  $\text{h}^\pm$ .
  - More results will come.
- 2022 measurement with (transversely polarised)  ${}^6\text{LiD}$  target just about to start.

These measurements provide important input to general understanding of the transverse-momentum-dependent structure of the nucleon and of the fragmentation process.

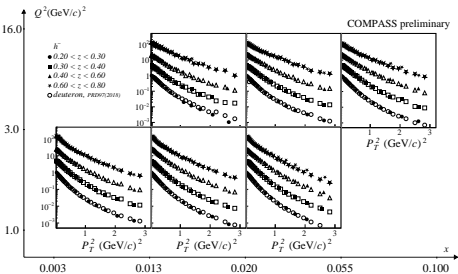
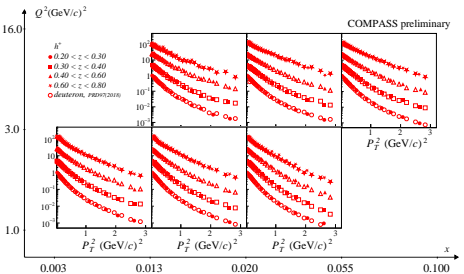
Thank you for your attention!

# Backup: Kinematic distributions on LH<sub>2</sub>



Normalised kinematic distributions: real data, LEPTO, HEPGEN  $\rho^0$  and HEPGEN  $\phi$ .

# Backup: Comparison of the $P_T$ -distributions with deuteron





# Backup: Distributions of $q_T$ and $q_T^2$

$$q_T = P_T/z$$

